Materials Sciences and Applications, **2011, 2, 1644-1653**
doi:10.4236/msa.2011.211219 Published Online November 2011 (http://www.SciRP.org/journal/msa)

Dispersibility, Shape and Magnetic Properties of Nano-Fe_3O_4 Particles

Xiaojuan Liang[1], Haowei Shi[2], Xiangchen Jia[2], Yuxiang Yang[2*], Xiangnong Liu[3]

[1]College of Chemistry and Materials Engineering, Wenzhou University, Wenzhou, China; [2]Department of Chemistry, East China University of Science & Technology, Nanjing, China; [3]Analysis Test Center, Yangzhou University, Yangzhou, China.
Email: *yxyang@ecust.edu.cn

Received July 25th, 2010; revised November 19th, 2010; accepted September 8th, 2011.

ABSTRACT

Nano-Fe_3O_4 particles were prepared by a two-step microemulsion method, the influence of molar ratio of water to NP-5 (R), alkali concentration and temperature on dispersibility and shape of the nanoparticles were discussed. Magnetic studies were also carried out using VSM in this paper. It was found that the optimum preparation parameters are R = 6.0, alkali concentration = 2.5 mol·L^{-1}, initial total iron concentration as 0.88 mol·L^{-1}, and the temperature being 30˚C, the prepared nano magnetite particles have uniform size and good dispersibility with a crystal structure belonging to cubic Fe_3O_4 and lattice parameters of a = 8.273 Å. The results of magnetic studies show, magnetic properties of particles are influenced by dispersibility of nanoparticles which depends on size of clusters. The better dispersibility of nanoparticles leads to more ordered inner magnetic vector, and so the stronger magnetic behavior of nano-Fe_3O_4 particles.

Keywords*: *Nano-Fe_3O_4 Particle*, *Dispersibility of Nanoparticles*, *Magnetic Properties*, *Saturation Magnetization

1. Introduction

Magnetic nanoparticles have been widely studied because of their fascinating properties and wide range of potential applications in ferrofluids, information storage, pigment, medicine, biomedical and bioengineering, etc. [1-3] The nano magnetite particles can be synthesized by precipitation from the solution of mixed Fe(II)/Fe(III) salts in alkaline medium. Besides this, many techniques have been used to synthesize magnetite such as thermal decomposition [4] hydrothermal synthesis [5], coprecipitation of an aqueous solution of ferrous and ferric ions by a base [6-8],oxidation of the ferrous hydroxide gels using KNO_3 [9], γ-ray irradiation [10], microwave plasma synthesis [11] sol-gel [12], nonaqueous route [13-15] etc. Many applications depend on their size and stoichiometry of particles, however the dispersibility and shape of prepared particles varies with the hydrolysis condition, the additive surfactant[4] and organic compound [5], most of them exhibit nano spherical particles [16-18].

Many reports have not systematically studied various factors affecting dispersibility and shape of nano-Fe_3O_4 particles, especially the relationship between dispersibility and their magnetic behavior. So in this paper, we report the preparation process of nano-Fe_3O_4 particles using two-step microemulsion method. The different factors affecting dispersibility of nano-Fe_3O_4 particles, including NaOH concentration, reaction temperature, water-surfactant ratio, and initial total iron concentration, are discussed. The relationship between the magnetic properties and dispersion behavior of nano-Fe_3O_4 particles is also studied.

2. Experimental

2.1. Synthesis of Nanoparticles Fe_3O_4

Surfactant NP-5, cosurfactant butanol, and kerosene were mixed in the ratio of 1:1:10, the muddy mixed solution was then stirred until a clear and transparent solution was obtained. The previous solution was divided into two parts of (1) and (2).

Firstly, the boiled deionized water was added to the solution of (1) with a ratio R (R is the molar ratio of water to NP-5), the microemulsion became clearer and clearer through stirring. Then certain amount of $FeCl_2·4H_2O$ and $FeCl_3·6H_2O$ were added into the microemulsion system with the molar ratio of Fe^{2+} to Fe^{3+} as 3:2 while vigorously stirring. The microemulsion labeled as (1) became brown-yellow and transparent.

Secondly, the boiled NaOH solution with the concen-

tration at 2.0 mol/L, 2.5 mol/L, 3.0 mol/L, and 3.5 mol/L were added to the solution of (2) with the corresponding ratio R value previously mentioned in above step, the microemulsion labeled as (2) became clear and transparent while stirring.

After stirring microemulsion (1) and (2) for 3 h, the microemulsion (2) was dropped into the microemulsion (1) with N_2 gas passing through, the brown-yellow solution immediately turned black. The mixed system was stirred for 3.0 h and left standing for 1 h at 80˚C. After that, the upper layer was transparent and the bottom layer was black, then the upper layer was discarded and the bottom layer was washed with absolute alcohol for twice. The obtained product was dried in a vacuum oven at 80˚C for 2 h, and calcined at 350˚C for 4 h, following the dry product was calcined in tube type electric-resistance furnace at 350˚C for 4 h. Eventually, the black powders were obtained.

2.2. Characterization of Nanoparticles Fe_3O_4

The x-ray diffraction pattern of the sample was recorded by D/max 2550 VB/PC x-ray diffractometer, using Ni-filtered with Cu Kα radiation (40 mA, 40 KV, 1˚(2θ) min^{-1}) at room temperature. The dispersibility and shape of samples were observed by Tecnai-12 transmission electron microscope (TEM) (120 KV).

3. Results and Discussions

Figure 1 shows the XRD patterns for magnetic particles prepared on the condition of R = 6.0 and C_{NaOH} = 2.5 mol/L, the X-ray diffraction patterns of magnetic particles all display sharp peak with strong diffraction intensity, and low background, the indices (220) and (400) labeled by red color are found to be corresponding to 2θ values of 31.4 and 45.4 respectively, in a good agreement with the JCPDS card 26 - 1136, which belongs to cubic system. However, the indices (220) and (400) labeled by blue color and the indices (311), (422), (511), (440), (620), (622) and (642) are corresponding to the standard diffraction card JCPDS 19-629(pure Fe_3O_4). It is demonstrated that the obtained products are mixture of two kinds of cubic nano-Fe_3O_4 particles, with corresponding JCPDS card being 19 - 629 and 26 - 1136 respectively.

The TEM images shown in **Figure 2** reveals the nanocrystallite nature of magnetite particles with a good dispersibility, the average particle size measured from the TEM images has been found to be 22 nm.

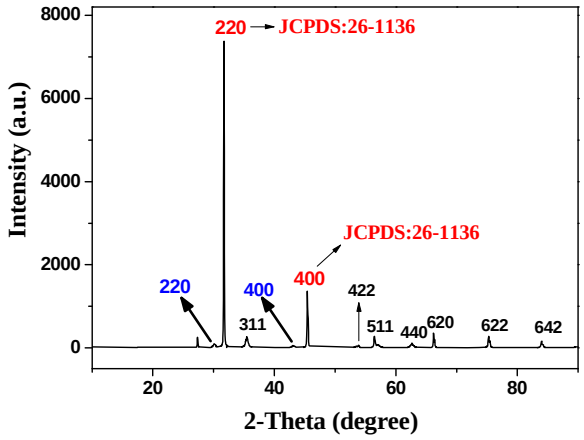

Figure 1. X-ray diffraction pattern of the nano magnetite.

3.1. Effect of Different NaOH Concentration on Magnetite Morphology

In the preparation, the alkali concentration and water-core of microemulsion are two chief factors that affect dispersibility of Fe_3O_4 particles. In order to discuss the effects of alkali concentration on the dispersibility and shape of Fe_3O_4 particles, we performed five experiments under alkaline condition at concentration of 1.5, 2.0, 2.5, 3.0 and 3.5 $mol \cdot L^{-1}$ respectively. The dispersibility of prepared magnetite was investigated by transmission electron microscope, five TEM images of magnetite are shown in **Figure 3**.

It is found when the concentration of NaOH is lower than 2.0 $mol \cdot L^{-1}$ the agglomerated granules appear in the prepared sample, and the spindle-like particles are formed. The image recorded in **Figure 3(a)** exhibits rod-like form with spindle-like form crossing over. It is because the precipitate of Fe^{3+} occurs at pH in the range of 3 - 4, which is calculated by $K^{0}_{sp,\,Fe(OH)3}$, but precipitate of Fe^{2+} occurs at pH in the range of 8 - 9 calculated by $K^{0}_{sp,\,Fe(OH)2}$, indicating the amount of NaOH for precipitate of Fe^{3+} is much less than that for precipitate of Fe^{2+}. So when the shortfall amount of NaOH is intro-

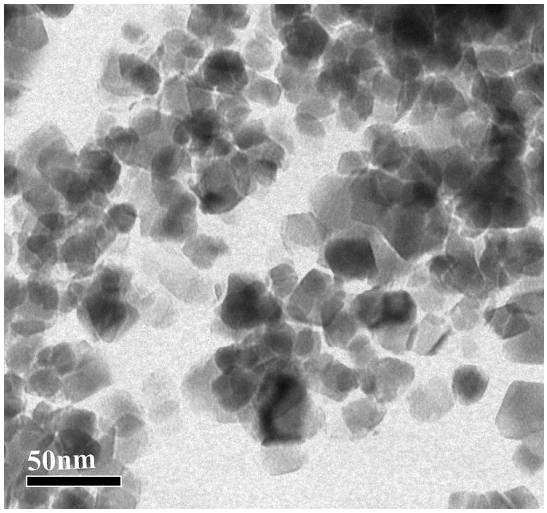

Figure 2. TEM morphology of the nano magnetite.

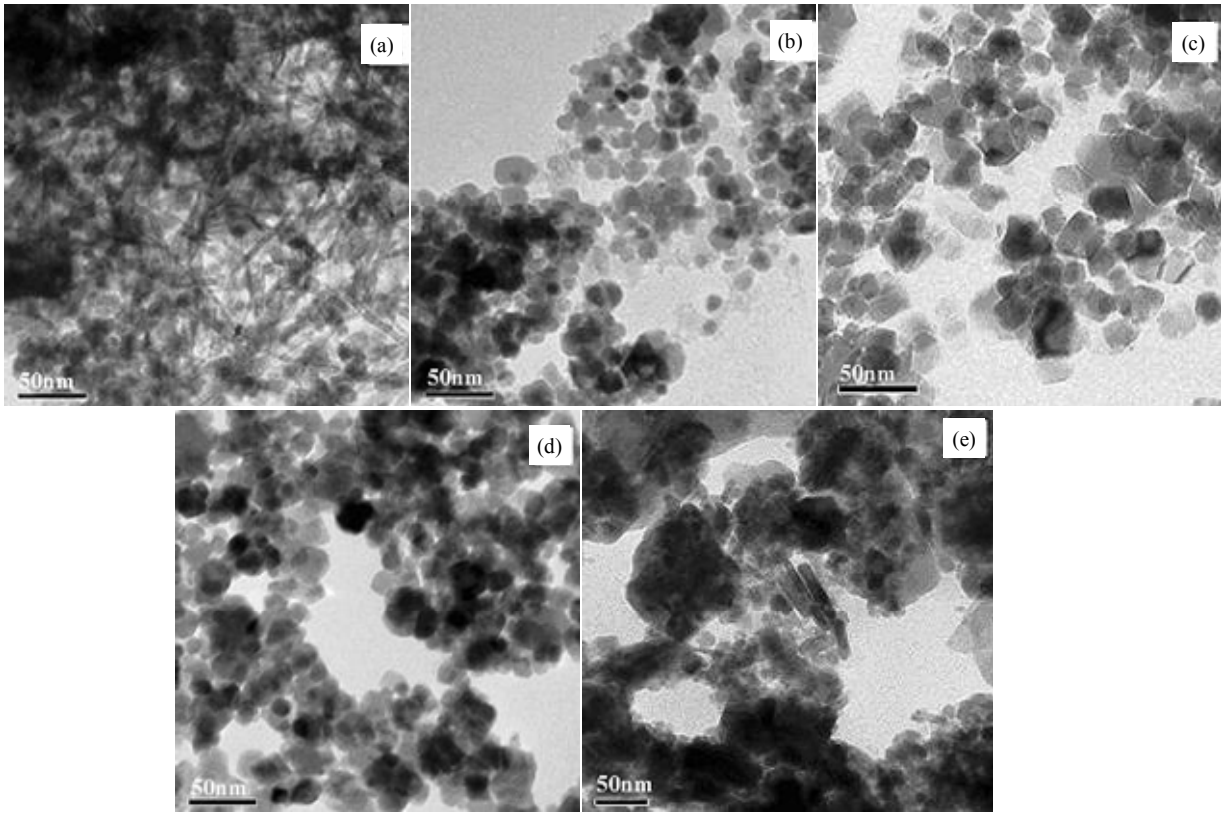

Figure 3. The morphology of Fe_3O_4 particles prepared under alkaline condition at concentration of (a) 1.5; (b) 2.0; (c) 2.5; (d) 3.0; (e) 3.5 mol/L.

duced into the mix solution containing Fe^{3+} and Fe^{2+} ions, the pH is measured about 7.5, the Fe^{3+} ions preferentially form precipitates by itself instead of co-precipitating with Fe^{2+} ions, the results are that more orange red FeOOH phase is formed first, but less Fe_3O_4 phase is formed.

When the concentration of NaOH reaches 2.0 mol·L^{-1} with the pH measuring about 8.5, the spherical particles and local agglomeration of granules are formed, as shown in **Figure 3(b)** The reason is that completely co-precipitation of Fe^{3+} with Fe^{2+} ions generally occur at pH above 9.2 as reported by reference [19]. So at the pH about 8.5, the Fe^{3+} ions begin to co-precipitate with the Fe^{2+} ions, and form the Fe_3O_4 phase. But this time, the residual Fe^{3+} ions hydrolyzes into tiny FeOOH particles, due to lower pH value than that of coprecipitation of Fe^{3+} with Fe^{2+} ions, as a result, the tiny FeOOH particles produced by hydrolysis easily form local agglomeration in the sample.

In contrast to **Figure 3(b)**, the image recorded in **Figure 3(c)** exhibit spherical form with well uniform sizes, its average size is measured about 22 nm. The experimental results demonstrate that the optimum NaOH concentration for coprecipitation of Fe^{3+} with Fe^{2+} ions is 2.5 mol/L, with the pH measuring above 9.2, the reaction mechanism can be inferred as the following:

$Fe^{2+} + Fe^{3+} + OH^- \rightarrow Fe(OH)_2/Fe(OH)_3$ (coprecipitation of Fe^{3+} with Fe^{2+})

$Fe(OH)_2 + Fe(OH)_3 \rightarrow FeOOH + Fe_3O_4$ ($pH \leq 7.5$)

$FeOOH + Fe^{2+} \rightarrow Fe_3O_4 + H^+$ ($pH \geq 9.2$)

Generally speaking, under the perfect condition, co-precipitation occurs when the mole ratio of Fe^{3+} to Fe^{2+} is 2:1. But actually, the Fe^{2+} is easily oxidized when exposed in air, so in this paper, the mole ratio of Fe^{3+} to Fe^{2+} is kept constant at 2:3. The whole coprecipitation equation of Fe^{3+} with Fe^{2+} can be written in the following:

$$Fe^{3+} + Fe^{2+} + 8OH^- \rightarrow Fe_3O_4 + 4H_2O$$

But when the concentration of NaOH becomes 3.0 mol·L^{-1}, slightly excessive amount of the NaOH makes particles form partial aggregates in the sample, and induces the particles increase in size. Its average size is measured larger than that of the image recorded in **Figure 3(c)**, as can be seen in the **Figure 3(d)**.

It is noted that when the pH of Fe^{3+} and Fe^{2+} solution exceeds pH of coprecipitation, the Fe^{3+} and Fe^{2+} ion all hydrolyze much fast and have strong tendency to precipitate. And pH increases with the concentration of NaOH increases, the excessive alkali leads to rapidly

growing in size of clusters with different shapes, and finally formation of agglomerated sphere particles in different sizes and shapes. The higher concentration of NaOH, the more heavily agglomeration, the results can be seen in the **Figure 3(e).**

3.2. Effect of Different Water/Surfactant Molar Ratio (R)

The size of water-core is dependent upon water/surfactant ratio (R) [20], when R keeps constant, the size of water-core keeps unchanged; but when R increases, the water-core grows in size; this will lead to many topological constructions. To study the effect of R on the dispersibility of nano-Fe_3O_4 particles, mole value of Fe^{3+} was fixed at 0.7 mmol, mole value of Fe^{2+} was fixed at 1.05 mmol, the concentration of NaOH fixed at 2.5mol/L, and R was controlled at 3, 5, 6 and 7.

As seen from **Figure 4**, the four prepared samples are heavily agglomerated shaped, local agglomerated shaped, well uniform spherical shaped and spheroidally aggregated shaped respectively. The results indicate that the distribution of the water-core in oil phase is chiefly determined by the water/surfactant molar ratio (R), the nucleation and growth of hydrolyzed core is likely to be a diffusion-controlled process through interaction between micelles. When R = 3.0, the image of nano-Fe_3O_4 particles exhibit heavily agglomerated shaped with average particle size measuring about 10 nm, because the low water/surfactant molar ratio leads to crowded dispersion of NP-5 in the microemulsion system, and so strong interaction between micelles of NP-5. This induces water-core contracting in the oil phase, the crystal core can only grow in the crowded medium, and form heavily agglomeration at last.

When R = 5.0, the increase of water/surfactant molar ratio leads to broader dispersion of NP-5 in the microemulsion system, and the water-core can be incompletely dispersed in the oil phase. As a result, the particle size increase, with the average size measuring about 20 nm, and a local agglomeration is formed. When R = 6.0, water-core is dispersed uniformly in the oil phase, and the crystal core grows regularly, the average particle size is measured about 22 nm, because the microemulsion system may form well dispersive micelle.

When R = 7.0, the high mole ratio of water/surfactant leads to a great increase in water-core size, which decreases the distance between neighbouring water-core, thus leading to an increase in contractive interactions between neighbouring water-core. The crystal core grows fast but irregularly in the uncrowded medium, and form

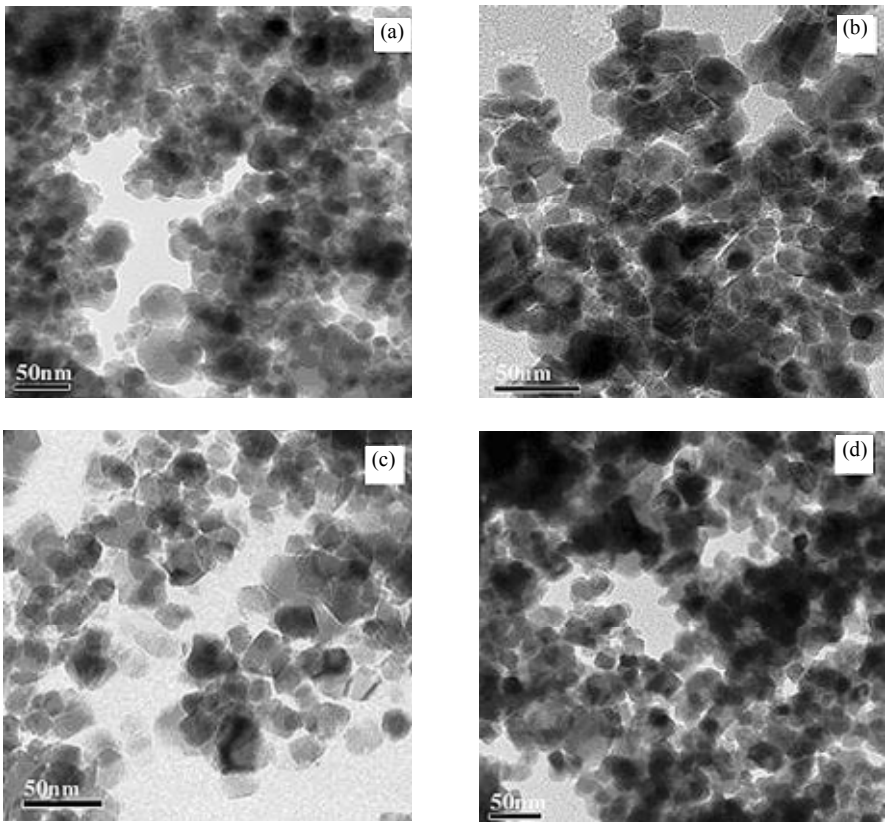

Figure 4. TEM images of nano-Fe_3O_4 particles under different R: (a) 3.0; (b) 5.0; (c) 6.0; (d)7.0.

aggregated spheroidally shaped particles.

3.3. Effect of Temperature on Magnetite Morphology

The dispersibility of magnetite is also depended upon the temperature for preparation. When the nano-Fe_3O_4 particles were prepared at 30˚C, the TEM image recorded in **Figure 5(a)** exhibits well dispersed particles with uniform size measuring about 10 - 20 nm. Upon increasing the synthesis temperature from 30 to 45˚C, the TEM image of **Figure 5(b)** has lower dispersion than the corresponding TEM image of **Figure 5(a)** of the sample prepared at 30˚C.

When the synthesis temperature continued to increase from 45˚C to 60 and 70˚C, particles with spherical and irregular shapes with some agglomeration are noted (**Figure 5(c)** and **Figute 5(d)**), chiefly due to rapid Brown movement of nano-Fe_3O_4 particles with temperature increasing. The increase in frequency of collision between the particles leads to kinetic energy of collision increaseing, this makes the nano-particles have strong tendency to overcome potential barrier between them, and agglomerate into large particles, as a result, a phenomenon of agglomeration takes place.

Throughout crystallite size variations of the nanosized nano-Fe_3O_4 particles, one can find that the particle sizes of synthesized products are increased with the synthesis temperature increasing, the particle sizes of synthesized products are 15 nm, 27.5 nm, 31 nm, and 36.5 nm, corresponding to the synthesis temperature being 30˚C, 45˚C, 60˚C, and 70˚C respectively.

3.4. Effect of Initial Total Iron Concentration on Magnetite Morphology

To study the effect of initial total iron concentration on the dispersibility of nano-Fe_3O_4 in the microemulsion system, R was maintained at 6.0, the concentration of NaOH maintained at 2.5 mol·L^{-1}, and the temperature was kept at 30˚C. The sample was synthesized by controlling initial total iron concentration at 0.63, 0.88, and 1.25 mol·L^{-1} (in water) respectively, while the mole ratio of Fe^{3+} to Fe^{2+} was kept constant at 2:3.

As seen from **Figure 6(a)**, the TEM image shows large amount of irregular rod particles with lengths about

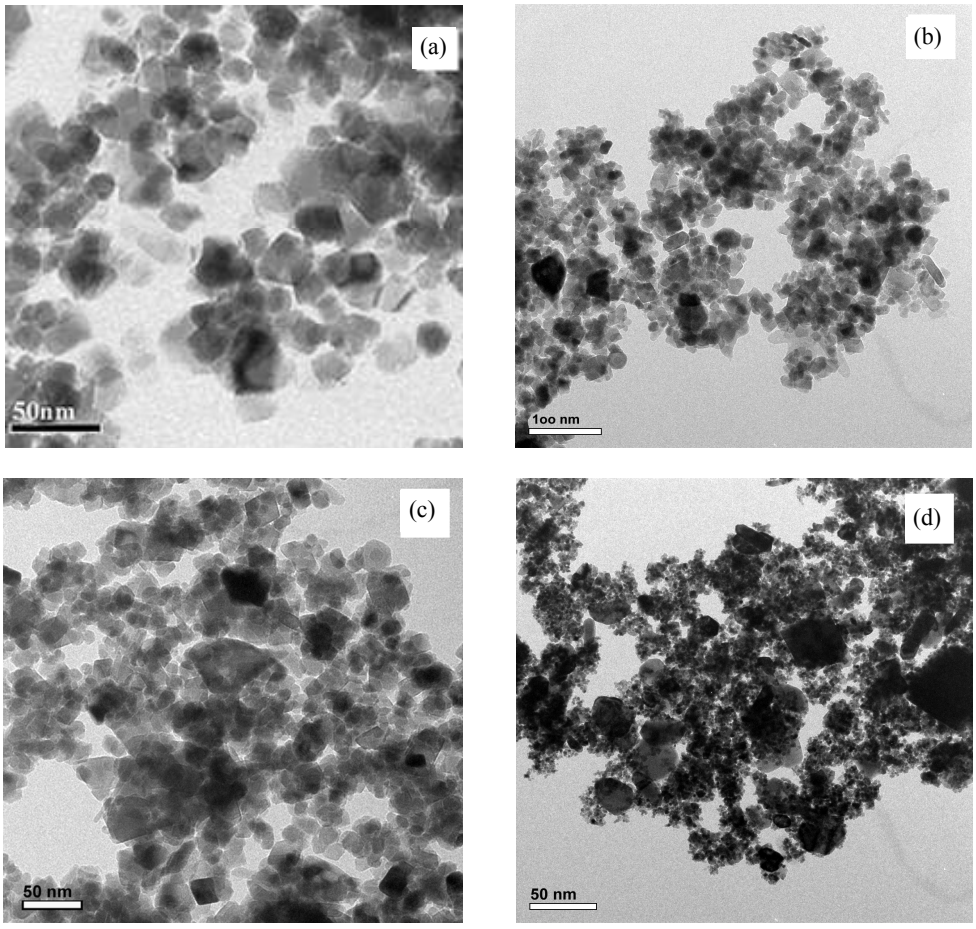

Figure 5. TEM images of nano-Fe_3O_4 particles at different temperature T: (a) 30˚C; (b) 45˚C; (c) 60˚C; (d) 70˚C.

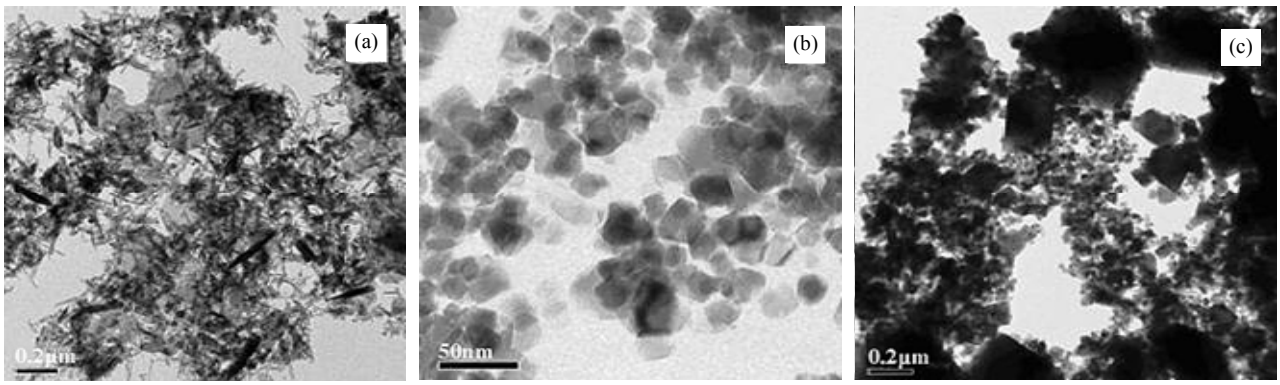

Figure 6. TEM images of nano-Fe_3O_4 particles at different initial total iron concentration CFe: (a) 0.63 mol/L; (b) 0.88 mol/L; (c) 1.25 mol/L.

100 - 250 nm when initial total iron concentration was at 0.63 mol/L, probably due to formation of β-FeOOH particles [20]. As we know, the Fe^{3+} ions is hydrolyzed much faster than the Fe^{2+} ions in alkaline solution according to $K^{\theta}_{sp,\ Fe(OH)3}$ and $K^{\theta}_{sp,\ Fe(OH)2}$, when the initial total iron concentration is low, the mole ratio of alkaline concentration $[OH^-]$ to initial total iron concentration $\{[Fe^{3+}] + [Fe^{2+}]\}$ becomes high, this induces Fe^{3+} ions hydrolyzing much fast, and forming β-FeOOH particles before coprecipitation with Fe^{2+} ions.

The dispersibility of nano-Fe_3O_4 in the microemulsion system is also found to be dependent on the initial total iron concentration and size of water-core. When water/surfactant ratio (R) is constant, the size of water-core cannot change, so dispersibility of nano-Fe_3O_4 are mainly depended on the dispersion of Fe^{3+} and Fe^{2+} ions in water-core. As seen from **Figure 6(b)**, the TEM image shows well uniform spherical shaped with lengths of 22 nm, probably because the Fe^{3+} and Fe^{2+} ions are dispersed uniformly in water-core when the initial total iron concentration was controlled at 0.88 mol·L^{-1}.

When the initial total iron concentration was controlled at 1.25 mol·L^{-1}, excessive Fe^{3+} and Fe^{2+} ions may not be dispersed uniformly in water-core. It makes the new-formed tiny crystal core mutually collide to become massive agglomeration before completely growing, thus hinders the growth of the tiny core, and so results in larger sized clusters of tiny particles formation, as can be seen in **Figure 6(c)**. By using the Scherrer formula and X-ray diffraction method, the particle diameter is measured to be 7 nm.

3.5. The Relationship between Magnetic Properties and Dispersion Behavior of Nano-Fe_3O_4 Particles

To study the effect of particle dispersibility on magnetic properties, five samples A, B, C, D and E were prepared under different conditions with constant temperature at 30˚C, while four samples A, A-2, A-3 and A-4 were prepared under different temperature conditions with constant R, alkaline concentration and total iron concentration. Listed in **Table 1** are the nomenclatures we used for different products as well as the alkaline concentration, total iron concentration and the temperature in their preparation.

Table 1. Preparation alkaline and total iron concentration for the products studied.

Products identifier	R	alkaline concentration	total iron concentration	
Sample A	6.0	2.5 mol·L^{-1}	0.88 mol·L^{-1}	T = 30˚C
Sample B	6.0	3.0 mol·L^{-1}	0.88 mol·L^{-1}	T = 30˚C
Sample C	6.0	3.5 mol·L^{-1}	0.88 mol·L^{-1}	T = 30˚C
Sample D	6.0	2.5 mol·L^{-1}	0.63 mol·L^{-1}	T = 30˚C
Sample E	6.0	2.5 mol·L^{-1}	1.25 mol·L^{-1}	T = 30˚C
Sample A-2	6.0	2.5 mol·L^{-1}	0.88 mol·L^{-1}	T = 45˚C
Sample A-3	6.0	2.5 mol·L^{-1}	0.88 mol·L^{-1}	T = 60˚C
Sample A-4	6.0	2.5 mol·L^{-1}	0.88 mol·L^{-1}	T = 70˚C

Table 2. The magnetic parameters of sample A, B, C, D and E.

Sample	Ms /(emu·g^{-1})	Mr /(emu·g^{-1})	Mr/Ms	H_C/Oe
A	62.8	12.6	0.20	105.3
B	14.5	1.63	0.11	81.28
C	13.7	2.11	0.15	126.3
D	10.0	1.72	0.17	92.27
E	22.1	3.13	0.14	126.3
A-2	34.0	3.2	0.094	65.5
A-3	33.8	2.3	0.068	37.3
A-4	21.2	1.4	0.066	29.2

Ms: saturation magnetization; Mr: remanent magnetization; Mr/Ms: squareness.

The dispersibility of nanoparticles was observed by transmission electron microscopy (TEM) with a Tecnai-12 transmission electron microscope operated at 120KV, as can be seen in the **Figures 3(c)-(e)**, **Figures 5(a)-(d)** and **Figures 6(a)-(c)**. It was shown that cluster size and cluster distribution can be influenced in a wide range (some order of magnitude) by the variation of the preparation parameters.

Magnetic studies were carried out using a vibrating sample magnetometer (VSM BHS-55) with fields up to 30 k Gauss at room temperature. The magnetic curves of the eight samples can be seen in **Figure 7**, all magnetic parameters are listed in **Table 2**. Magnetic properties such as saturation magnetization, coercivity and squareness are discussed as following.

1) Saturation magnetization

Saturation magnetization represents magnetic intensity of magnetic materials. The magnetization curves of sample A, B and C shown in the **Figure 7** display magnetic properties of nano-Fe_3O_4 particles prepared with different alkaline concentration of 2.5, 3.0 and 3.5 mol·L^{-1} respectively. Whereas the magnetization curves of sample A, D and E shown in the **Figure 7** display magnetic properties of nano-Fe_3O_4 particles prepared with different initial total iron concentration at 0.88, 0.63 and 1.25 mol·L^{-1} respectively. The magnetization curves of sample A, A-2, A-3 and A-4 shown in the **Figure 7** display magnetic properties of nano-Fe_3O_4 particles prepared with different temperature at 30˚C, 45˚C, 60˚C and 70˚C respectively. By comparing magnetic parameters of samples listed in **Table 2** with their dispersibility shown in **Figures 3(c)-(e)**, we obtain that sample A shows the strongest saturation magnetization, chiefly due to its uniform size and best dispersion behavior. It is under alkaline condition of concentration at 2.5 mol·L^{-1}, that coprecipitation of Fe^{3+} with Fe^{2+} ions can occur. The saturation magnetization decreases to some extent with gradual increase of NaOH concentration from 2.5 mol·L^{-1} to 3.5 mol·L^{-1}. Because the nano-Fe_3O_4 particles change from well-dispersed into partial aggregate, and finally heavily agglomerate, with an increase of alkaline concentration.

The better dispersibility of nanoparticles can be explained by the size of clusters with uniform shape. Excessive alkali induces the Fe^{3+} and Fe^{2+} ions all hydrolyzing much fast, leads to nanoparticles rapidly changing into larger sized clusters with arbitrary smaller shaped particles. The better dispersibility of nanoparticles, the stronger magnetic behavior of them [21]. This means inner magnetic vector becomes more ordered, with an increase of dispersion of nanoparticles, and thus the nanoparticles display stronger magnetism, leading to an increase of saturation magnetizationσs.

When different initial total iron concentration was adopted during preparation, the saturation magnetization of particles is found to be stronger with increase of total iron concentration. For sample D, the total iron concentration is so low that Fe^{3+} ions hydrolyzed faster than Fe^{2+} ions and formed β-FeOOH particles before coprecipitation with Fe^{2+} ions. This would lead to decrease of its saturation magnetization. In the opposite side, when the total iron concentration was higher than 0.88 mol·L^{-1}, coprecipitation of Fe^{3+} with Fe^{2+} ions occurs, this prevents β-FeOOH particles from generating, causing an increase of saturation magnetization σs of sample E. But mutually collision between new-formed tiny crystal cores hinders the growth of the tiny core, leading to formation of larger sized clusters with different tiny shapes. So dispersibility of nanoparticles of sample E is worse than that of sample A, inner magnetic vector becomes less ordered also, as a result, the saturation magnetization σs of sample E becomes lower than that of sample A.

By comparing magnetic parameters of samples listed in **Table 2** with their dispersibility shown in **Figures 5 (a)-(d)**, we obtain that sample A shows the strongest saturation magnetization, also chiefly due to its uniform size and best dispersion behavior. When the nano-Fe_3O_4 particles were prepared at 30˚C, the sample A was observed to have the best dispersibility, when the temperature increased from 30˚C to 70˚C, the dispersibility of the sample A-2, sample A-3 and ample A-4 decreased steadily, resulting in inner magnetic vector getting less ordered [21], and thus a progressive decrease in the saturation magnetization σs for sample A-2, sample A-3 and sample A-4.

The above results demonstrate that saturation magnetization of nano-Fe_3O_4 particles is greatly influenced by dispersion properties and their shapes. The better dispersed nano-Fe_3O_4 particles with more uniform and dispersed shapes will have higher saturation magnetization, and thus display stronger magnetism.

2) Coercivity

Coercivity of magnetic matericals mainly depends on anisotropy, saturation magnetization and corresponding structure parameters. Covercivity which depends on magneto-crystalline anisotropy can be expressed by the following formula according to Zhou.[22]:

$$Hc = 2K/\mu_0 \cdot Ms$$

In this formula, K value depends only on property of material itself, but not related to particle size and shape, it is inversely proportional to saturation magnetization. As seen from **Table 2**, coercivity of sample A is higher than that of sample B and D, but lower than that of sample C and sample E.

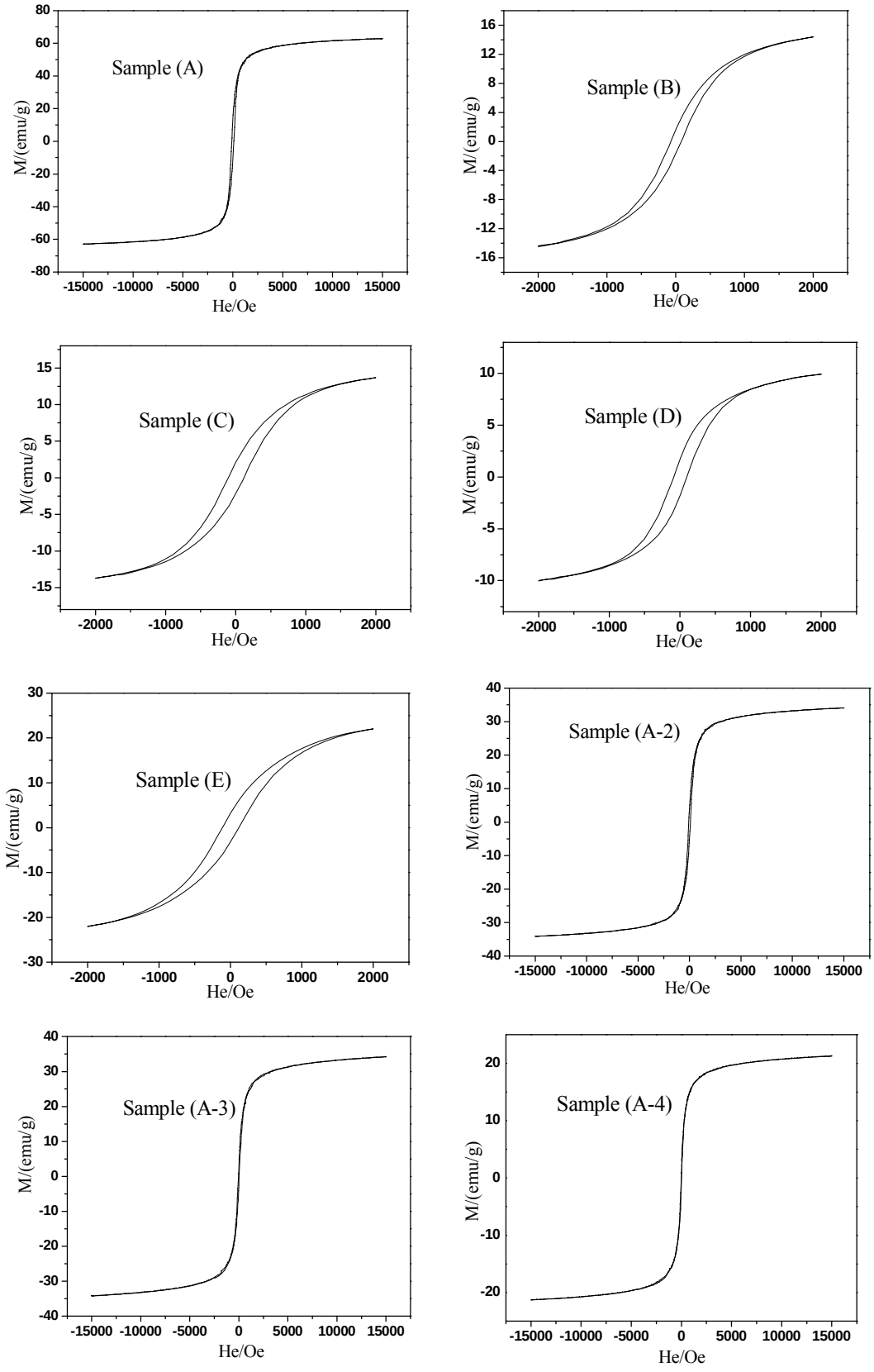

Figure 7. Magnetization hysteresis curves of nano-Fe_3O_4 particles synthesized under different conditions.

According to the formula, sample A should have the lowest coercivity compared with other samples because of its highest saturation magnetization. However, it is found that there is no such obvious linear relationship between coercivity and saturation magnetization. The coercivity of particles is related to their size of clusters and shapes. It is noted that coercivity decreased with reduction of particle size below 40nm [23]. As shown in **Figures 3(d)-(e)** and **Figures 6(a)-(c)**, sample A shows well uniformly spherical shaped with lengths of 22 nm, but both of samples C and E display large size of clusters, but consisting of smaller size particles than sample A. So both of samples C and E show larger coercivity than sample A. On the other hand, average size of sample B is larger than that of sample A, and sample D is 100 - 250 nm length irregular rod particles, these all lead to sample A having a larger coercivity than the sample B and D.

As shown in **Figures 5(a)-(d)**, with an increase of temperature from 30˚C to 70˚C, the dispersibility of the sample decreased progressively, resulting in the coerciveity of sample decreasing. A plot of coercivity versus the temperature is shown in **Figure 8**, the **Figure 8** shows linear relationship between coercivity and temperature. It demonstrates that the temperature has significant influence on the anisotropy and dispersibility of the sample, with an increase of temperature, the anisotropy and dispersibility of the sample decreases, leading to coercivity decreasing.

3.6. Indexing the Powder X-Ray Diffraction Pattern

The results of indexing the powder X-ray diffraction pattern are listed in **Table 3**. **Table 3** shows that all the diffraction peaks in the pattern can be readily indexed by one set of lattice parameters. The largest relative deviation between the calculated D_{cal} and experimental D_{exp} is less than 0.347%, which indicates that the synthesized products are a single phase with cubic structure. The crystal structure of synthesized product belongs to the cubic system.

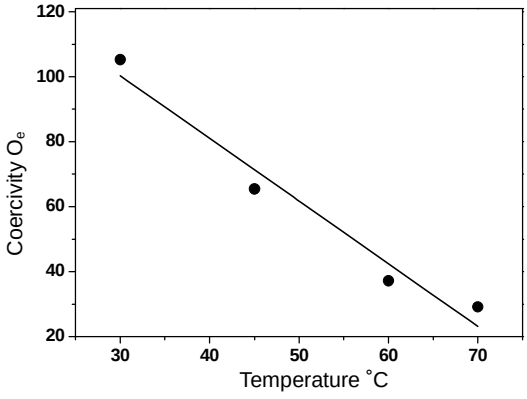

Figure 8. Plot of coercivity versus the temperature.

Table 3. The experimental data and the calculated results for powder X-ray diffraction pattern of the nano-Fe_3O_4 particles cubic system: a = 8.273 Å.

D_{exp} (Å)	D_{cal} (Å)	h k l	I(%)	D_{exp} (Å)	D_{cal} (Å) (nm)	h k l	I(%)
2.8430	2.9249	220	100	1.4846	1.4625	4 4 0	1.89
2.5266	2.4944	311	3.71	1.4113	1.3081	6 2 0	4.33
1.9977	2.0682	4 00	18.91	1.2622	1.2472	6 2 2	3.08
1.7008	1.6887	4 2 2	1.27	1.1522	1.1055	6 4 2	1.89
1.6287	1.5921	5 1 1	3.71				

4. Conclusions

In summary, the cubic nano-Fe_3O_4 particles have been successfully synthesized by using two-step microemulsion method. The dispersibility, shape and anisotropy of nano-Fe_3O_4 particles vary with R value, alkali concentration, and the temperature. The prepared nano-Fe_3O_4 particles all exhibits dispersive spherical form with well uniform sizes measured about 22 nm under condition of R = 6.0, alkali concentration at 2.5 mol/L, with the temperature at 30˚C. Magnetic properties are influenced greatly by dispersibility and shape of particles. The crystal structure of the nano-Fe_3O_4 particles belongs to cubic system with lattice parameters (a = 8.273 Å).

5. Acknowledgements

We thank the National Natural Science Foundation of China (No: 20971043), and the financial support from Wenzhou science and technology project (G2010071).

REFERENCES

[1] V. E. Fertman, "Magnetic Fluids Guide-Book: Properties and Applications," Hemisphere Publishing Co., New York, 1990.

[2] A. Kondo and H. Fukuda, "Preparation of Thermosensitive Magnetic Microspheres and their Application to Bioprocesses," *Colloids and Surfaces A*: *Physicochemical and Engineering*, Vol. 153, 1999, pp. 435-438. doi:10.1016/S0927-7757(98)00465-8

[3] D. G. Shchukin, I. L. Radtchenko and G. B. Sukhorukov, "Micron-Scale Hollow Polyelectrolyte Capsules with Nano-Sized Magnetic Fe_3O_4 Inside," *Materials Letters,* Vol. 57, 2003, pp. 1743-1747. doi:10.1016/S0167-577X(02)01061-3

[4] B. Gržeta, M. Ristić, I. Nowik and S. Musić, "Formation of Nanocrystalline Magnetite by Thermal Decomposition of Iron Choline Citrate," *Journal of Alloys and Compounds*, Vol. 334, 2002, pp. 304-312. doi:10.1016/S0925-8388(01)01792-3

[5] T. J. Daou, G. Pourroy, S. Bégin-Colin, J. M. Grenèche, C. Ulhaq-Bouillet, P. Legaré, P. Bernhardt, C. Leuvrey and G. Rogez, "Hydrothermal Synthesis of Monodisperse Magnetite Nanoparticles," *Chemistry Materials*, Vol. 18, 2006, pp. 4399-4404. doi:10.1021/cm060805r

[6] T. Sugimoto and E. Matijevic, "Formation of Uniform Spherical Magnetite Particles by Crystallization from Ferrous Hydroxide Gels," *Journal of Colloid and Interface Science*, Vol. 74, 1980, pp. 227-243. doi:10.1016/0021-9797(80)90187-3

[7] Y. S. Kang, S. Risbud, J. F. Rabolt and P. Stroeve, "Synthesis and Characterization of Nanometer-Size Fe_3O_4 and γ-Fe_2O_3 Particles," *Chemistry Materials*, Vol. 8, 1996, pp. 2209-2211. doi:10.1021/cm960157j

[8] T. Fried, G. Shemer, G. Markovich, "Ordered Two-Dimensional Arrays of Ferrite Nanoparticles," *Advanced Materials*, Vol. 13, 2001, pp. 1158-1161. doi:10.1002/1521-4095(200108)13:15<1158::AID-ADMA1158>3.0.CO;2-6

[9] G. Visalakshi, G. Venkataswaran, S. K. Kulshreshtha and P. N. Moorthy, "Compositional Characteristics of Magnetite Synthesised from Aqueous Solutions at Temperatures Upto 523K," *Materials Research Bulletin*, Vol. 28, 1993, pp. 829-836. doi:10.1016/0025-5408(93)90024-8

[10] S. Wang, H. Xin and Y. Qian, "Preparation of Nanocrystalline Fe_3O_4 by γ-ray Radiation," *Materials Letters*, Vol. 33, 1997, pp. 113-116. doi:10.1016/S0167-577X(97)00077-3

[11] D. Vollath and D. V. Szabo, "Synthesis and Magnetic Properties of Nanostructured Maghemite," *Journal of Materials Research*, Vol. 12, 1997, pp. 2175-2182. doi:10.1557/JMR.1997.0291

[12] C. Feldmann and H. O. Jungk, "Polyol-Mediated Preparation of Nanoscale Oxide Particles," *Angewandte Chemie International Edition*, Vol. 40, 2001, pp. 359-362. doi:10.1002/1521-3773(20010119)40:2<359::AID-ANIE359>3.3.CO;2-2

[13] S. Sun and H. J. Zeng, "Size-Controlled Synthesis of Magnetite Nanoparticles," *Journal of the American Chemical Society*, Vol. 124, 2002, pp. 8204-8205. doi:10.1021/ja026501x

[14] N. Pinna, S. Grancharov, P. Beato and P. Bonville, "Magnetite Nanocrystals: Nonaqueous Synthesis, Characterization, and Solubility," *Chemistry Materials*, Vol. 17, 2005, pp. 3044-3049. doi:10.1021/cm050060+

[15] Z. Li, H. Chen, H. Bao and M. Gao, "One-Pot Reaction to Synthesize Water-Soluble Magnetite Nanocrystals," *Chemistry Materials*, Vol. 16, 2004, p. 1391. doi:10.1021/cm035346y

[16] Y. H. Zhu and Q. F. Wu, "Synthesis of Magnetite Nanoparticles by Precipitation with Forced Mixing," *Journal of Nanoparticle Research*, Vol. 1, 1999, pp. 393-396. doi:10.1023/A:1010091625981

[17] Z. L. Liu and X. Wang, "Synthesis of Magnetite Nanoparticles in W/O Microemulsion," *Journal of Materials Science*, Vol. 39, 2004, pp. 2633-2636. doi:10.1023/B:JMSC.0000020046.68106.22

[18] M. D. Alcalá, J. M. Criado and C. Real, "Synthesis of Nanocrystalline Magnetite by Mechanical Alloying of Iron and Hematite," *Journal of Materials Science*, Vol. 39, 2004, pp. 2365-2370. doi:10.1023/B:JMSC.0000019998.78644.74

[19] L. X. Song, Z. Y. Lu, D. C. Liu, S. B. Cui and X. Q. Xiao, "Preparation of Magnetic Nanometer Fe3O4 with the Method of Complex Compound-Hydrolyzation Deposition," *Chemical industry and engineering progress*, Vol. 25, No. 1, 2006, pp. 54-55.

[20] Y. X. Yang, X. N. Liu, H. Zhu, Z. Huang, Y. R. Chen and Z. Y. Zhou, "Synthesis of β-FeOOH with Microemulsion," *Materials Science and Technology*, Vol. 23, No. 6, 2007, pp. 641-645. doi:10.1179/174328407X179665

[21] X. J. Liang, H. Zhu, Y. X. Yang, X. N. Liu, Y. R. Chen and H. P. Ying, "A Study on Synthesis of γ-Fe_2O_3 Powder and Magnetism Enhancement," *Acta Chimaca Sinica*, Vol. 64, No. 23, 2006, pp. 2351-2356.

[22] Z. G. Zhou, "The Ferrite," Science Press, Beijing, 1981.

[23] A. Manaf, R. A. Buckley, H. A. Davies, M. Leonowicz, "Enhanced Magnetic Properties in Rapidly Solidified Nd-Fe-B Based Alloys," *Journal of Magnetism and Magnetic Materials*, Vol. 101, 1991, pp. 360-362. doi:10.1016/0304-8853(91)90779-A

[24] L. L. Wang, "Study of Magnetic Properties of Ni-Fe-P and Ni-Fe-P-B Chemical Films," *Journal of Materials Review*, Vol. 15, No. 3, 2001, pp. 65-67.

